
Nash: Neural Adaptive Shrinkage for Structured High-Dimensional Regression

William R.P. Denault

Department of Human Genetics
University of Chicago
Chicago, IL
wdenault@uchicago.edu

Abstract

Sparse linear regression is a fundamental tool in data analysis. However, traditional approaches often fall short when covariates exhibit structure or arise from heterogeneous sources. In biomedical applications, covariates may stem from distinct modalities or be structured according to an underlying graph. We introduce *Neural Adaptive Shrinkage* (Nash), a unified framework that integrates covariate-specific side information into sparse regression via neural networks. Nash adaptively modulates penalties on a per-covariate basis, learning to tailor regularization without cross-validation. We develop a variational inference algorithm for efficient training and establish connections to empirical Bayes regression. Experiments on real data demonstrate that Nash can improve accuracy and adaptability over existing methods.

1 Introduction

Regularization techniques for linear models have been central in data analysis for decades [Hoerl and Kennard, 1970, Tibshirani, 1996, Zou and Hastie, 2005]. They remain central in modern data analysis as they are competitive approaches when the sample size is limited and the covariates are high-dimensional [Horvath and Raj, 2018, Bohlin et al., 2016, Horvath and Raj, 2018, Haftorn et al., 2021]. Despite their popularity, these methods often fall short when dealing with heterogeneous covariates that exhibit structural properties, such as nominal, ordinal, spatial, or graphical data. Classical regularization methods like Lasso [Tibshirani, 1996] typically apply uniform penalties across all covariates, which can be suboptimal when diverse predictor types are present in the covariate matrix (e.g. different genetic modalities). Real-world problems often benefit from tailored regularization that leverages the covariate side information, such as geographical proximity [Devriendt et al., 2021] or type biological measurements [Boulesteix et al., 2017]. On the other hand, the existing methods that leverage covariate side information [Tibshirani et al., 2005, Yuan and Lin, 2006, Yu et al., 2016, Boulesteix et al., 2017] are often limited by their application-specific nature and reliance on cumbersome cross-validation for hyperparameter selection [Tibshirani et al., 2005, Yuan and Lin, 2006].

In this work, we introduce *neural adaptive shrinkage* (Nash), a novel regression model framework that can leverage neural networks to automatically learn the form of the penalty and select the amount of regularization without using cross-validation or approximate methods. Hence, alleviating the limitations listed above. We fit Nash using a novel variational inference empirical Bayes (VEB) method called split VEB, originally introduced for smoothing over-dispersed Poisson counts [Xie, 2023], that we adapt here for high-dimensional Gaussian linear models. When no side information is available, our approach corresponds to optimizing the lower bound of a recently proposed model by Kim et al. [2024] and has similar computation complexity $O((n + K)p)$. However, our learning

algorithm is much simpler than the one proposed by Kim et al. [2024] and allows easy integration of machine learning approaches for penalty learning (e.g., neural net, xgboost Chen and Guestrin [2016]). Hence, Nash is both an extremely efficient high-dimensional regression method when no side information is present and a very flexible alternative when side information is available. We demonstrate that Nash is a highly competitive framework through a comprehensive study on real data examples.

2 Previous works and contribution

Previous works have mostly focused on two main types of side information on the covariate. The first type corresponds to groups (e.g. DNA methylation vs genotype data [Boulesteix et al., 2017]) or hierarchical information on the covariate; these works include group Lasso [Yuan and Lin, 2006] and other of its variations [Gertheiss and Tutz, 2010, Tutz and Oelker, 2017, Oelker and Tutz, 2017] and the IPF Lasso [Boulesteix et al., 2017]. Essentially, these methods extend classical regularized techniques for linear models by using different additive sub-penalties that depend on the group/hierarchy of the covariates. The second type of covariate side information leveraged in penalized regression is graphs [Tibshirani et al., 2005, Tibshirani and Taylor, 2011]. Spanning from simple L0 graph filtering problem such as Fused Lasso [Tibshirani et al., 2005] to more complex graphical structure that can be handled by the GEN Lasso [Tibshirani and Taylor, 2011] and more recent variations [Yu et al., 2016, Devriendt et al., 2021] that can fit a mix of the different penalties above within a single framework.

Our contribution. While combining neural networks with linear regression is not new [Okoh et al., 2018, Nalisnick et al., 2019, Lemhadri et al., 2021], existing methods focus on hybrid models [Okoh et al., 2018, Nalisnick et al., 2019] or learning link functions [Lemhadri et al., 2021] rather than learn the penalty itself. Our work differs substantially from the previous works listed above. To our knowledge, this is the first work to propose the use of a neural network to incorporate covariate side information when learning the penalty function in linear regression. Our work is much more assumption-lean compared to previous works, as Nash can leverage any side information that is processable by a neural net. Additionally, we propose a novel low-complexity variational approximation for empirical Bayes in multiple linear regression. The resulting learning algorithm is a simple and effective iterative procedure, akin to ADMM or proximal algorithms [Polson et al., 2015].

3 Problem definition

3.1 Variational Empirical Bayes for the Nash Model

The Nash model is defined as follows:

$$\mathbf{y} | \mathbf{X}, \beta, \sigma^2 \sim N(\mathbf{X}\beta, \sigma^2) \tag{1}$$

$$\beta_j \sim N(b_j, \sigma_0^2) \tag{2}$$

$$b_j \sim g(\mathbf{d}_j, \boldsymbol{\theta}) \tag{3}$$

where \mathbf{y} is a response vector of length n , \mathbf{X} is an $n \times p$ matrix, where p can be much larger than n (i.e., $p \gg n$), and \mathbf{x}_j is the j^{th} column of \mathbf{X} . The terms $\sigma^2 > 0$ and $\sigma_0^2 > 0$ are strictly positive variance parameters. The vector \mathbf{d}_j corresponds to side information on column j . The function $g(\cdot, \cdot)$ belongs to a certain class of functions \mathcal{G} and takes \mathbf{d}_j (side information) as its first argument and $\boldsymbol{\theta}$ (parameters) as its second argument. For any tuple $(\mathbf{d}_j, \boldsymbol{\theta})$, $g(\mathbf{d}_j, \boldsymbol{\theta})$ defines a distribution with a density, denoted as $g(b_j; \mathbf{d}_j, \boldsymbol{\theta})$ at the point b_j .

For simplicity, we assume that \mathbf{y} is scaled, centered with unit variance, and similarly that each columns of \mathbf{X} (i.e., $\|\mathbf{x}_j\| = 1$ and $\mathbb{E}(x_j) = 0$ for all $j = 1, \dots, p$). Note that we do not model the intercept in (1), as centering \mathbf{y} and \mathbf{X} prior to model fitting accounts for it, and it is straightforward to recover the effect for the unscaled \mathbf{X} [Chipman et al., 2001].

We assume that for each predictor \mathbf{x}_j in \mathbf{X} , we observe some side information \mathbf{d}_j . We intentionally remain vague on the form of the side information \mathbf{d}_j , with the only constraint being that $\mathbf{d}_1, \dots, \mathbf{d}_p$ can be processed by a neural network (e.g., images, tokens, graph matrices). For ease of presentation, we assume that we can store $\mathbf{d}_1, \dots, \mathbf{d}_p$ in a matrix \mathbf{D} of size $p \times k$. The case without any side information can be recovered by setting $\mathbf{d}_1 = \mathbf{d}_2 = \dots = \mathbf{d}_p$, i.e., constant side information.

Assuming that σ^2 and σ_0^2 are known, solving (1) in an Empirical Bayes (EB) fashion involves the following steps:

1. Learning the parameter $\boldsymbol{\theta}$ of the function $g(\cdot, \cdot) \in \mathcal{G}$ via maximum marginal likelihood $\mathcal{L}(\boldsymbol{\theta})$

$$\hat{\boldsymbol{\theta}} = \underset{\boldsymbol{\theta}}{\operatorname{argmax}} \mathcal{L}(\boldsymbol{\theta}) \quad (4)$$

$$= \underset{\boldsymbol{\theta}}{\operatorname{argmax}} \int p(\mathbf{y}|\mathbf{X}, \boldsymbol{\beta}, \sigma^2) \prod_j p(\beta_j|b_j, \sigma_0^2) g(b_j; \mathbf{d}_j, \boldsymbol{\theta}) db_j \quad (5)$$

2. Compute the posterior distribution

$$p_{\text{post}}(\boldsymbol{\beta}, \mathbf{b}) = p(\boldsymbol{\beta}, \mathbf{b}|\mathbf{y}, \mathbf{X}, \mathbf{D}, \sigma^2) \propto p(\mathbf{y}|\mathbf{X}, \boldsymbol{\beta}, \sigma^2) \prod_j p(\beta_j|b_j, \sigma_0^2) g(b_j; \mathbf{d}_j, \hat{\boldsymbol{\theta}}) \quad (6)$$

Wang and Stephens [2021] and Kim et al. [2024] study similar problems in the case where g does not depend on side information \mathbf{d} (i.e., $g(\mathbf{d}_j, \boldsymbol{\theta}) = g(\boldsymbol{\theta})$ for all j). They note that even in this case, both steps described above are computationally intractable except in some very special cases. This problem becomes even more challenging when we allow the prior g to depend on side information.

3.2 Split Variational inference

Given that we aim to fit model (1) in a tractable and efficient way, we propose fitting (1) via split VEB [Xie, 2023] using a candidate posterior of the form:

$$q(\boldsymbol{\beta}, \mathbf{b}) = \prod_j^P q_{\beta_j}(\beta_j) q_{b_j}(b_j) \quad (7)$$

The main idea behind split VEB is to decouple the prior/penalty learning step (step 1) from the posterior computation step (step 2). Our primary quantity of interest is the posterior of \mathbf{b} . However, using \mathbf{b} directly in the linear predictor results in a coupled prior/posterior update as in Kim et al. [2024]. To alleviate this problem, we essentially introduce a latent variable $\boldsymbol{\beta}$ that allows splitting the objective function into two parts that are separately updated (see equation 8). At a high level, split VEB allows deriving a coordinate ascent that essentially iterates between solving two simple problems in the spirit of splitting techniques used in optimization (e.g., ADMM or proximal algorithms Polson et al. [2015]).

Form of the ELBO Using the candidate posteriors of the form 7 leads to an ELBO of the following form for the Nash model

$$F(q_{\boldsymbol{\beta}}, q_{\mathbf{b}}, g, \sigma^2, \sigma_0^2)_{\text{Nash}} = \sum_i \mathbb{E} \log \frac{p(y_i|\mathbf{x}_i, \boldsymbol{\beta}, \sigma^2)}{q_{\boldsymbol{\beta}}(\boldsymbol{\beta})} + \sum_j \mathbb{E} \log p(\beta_j|b_j, \sigma_0^2) + \sum_j \mathbb{E} \log \frac{g(b_j; \mathbf{d}_j, \boldsymbol{\theta})}{q_{b_j}(b_j)} \quad (8)$$

High-Level Coordinate Ascent Update for Nash Let $\bar{\beta}_j = \mathbb{E}_q(\beta_j)$ denote the expected value of β_j with respect to q , and $\bar{b}_j = \mathbb{E}_q(b_j)$ denote the expected value of b_j . We define $\bar{\mathbf{r}} = \mathbf{y} - \mathbf{X}\bar{\boldsymbol{\beta}}$ as the vector of expected residuals with respect to q . Let \mathbf{X}_{-j} be the design matrix excluding the j^{th} column, and q_{-j} denote all factors $q_{j'}$ except factor j . The expected residuals accounting for the linear effect of all variables other than j are given by:

$$\bar{\mathbf{r}}_j = \mathbf{y} - \mathbf{X}_{-j}\bar{\boldsymbol{\beta}}_{-j} = \mathbf{y} - \sum_{j' \neq j} \mathbf{x}_{j'} \bar{\beta}_{j'} \quad (9)$$

1. **Update for $q_{\beta_j}^*$** : the coordinate ascent update $q_{\beta_j}^* = \arg \max_{q_{\beta_j}} F_{\text{Nash}}(g, q, \sigma^2, g, q, \sigma_0^2)$ is obtained by computing the posterior using

$$p(\bar{\mathbf{r}}_j|\mathbf{x}_j, \beta_j, \sigma) p(\beta_j|\bar{b}_j, \sigma_0^2)$$

This is a simple posterior computation due to conjugacy and has a closed form that only requires computing the ordinary least square (OLS) regression of \mathbf{x}_j on $\bar{\mathbf{r}}_j$ (see section 3.2.1).

2. **Update for (g^*, q_b^*) :** The coordinate ascent update

$$(g^*, q_b^*) = \arg \max_{g, q_b} F(q_\beta, q_b, g; \sigma^2)_{\text{Nash}}$$

is obtained by fitting a neural net with the following objective function:

$$\hat{\theta} = \arg \max_{\theta} \mathcal{L}(\theta) \quad (10)$$

$$= \arg \max_{\theta} \prod_{j=1}^p \int \mathcal{N}(\bar{\beta}_j; b_j, \sigma_0^2) g(b_j; \mathbf{d}_j, \theta) db_j \quad (11)$$

Then, by computing the posterior of

$$p(b_j | \bar{\beta}_j, \mathbf{d}_j, \sigma_0^2) \propto \mathcal{N}(\bar{\beta}_j; b_j, \sigma_0^2) g(b_j; \mathbf{d}_j, \hat{\theta})$$

for each b_j , which is also a simple posterior computation.

3. **Update for σ^2, σ_0^2**

$$(a) (\sigma^2)^* = \arg \max_{\sigma^2} F(q_\beta, q_b, g, \sigma^2, \sigma_0^2)_{\text{Nash}}$$

$$(b) (\sigma_0^2)^* = \arg \max_{\sigma_0^2} F(q_\beta, q_b, g, \sigma^2, \sigma_0^2)_{\text{Nash}}$$

The first step is a direct consequence of the work by Kim et al. [2024] (see Appendix for more details), the second step results from our splitting approach, and the last step is a standard coordinate ascent variational inference (CAVI) step. We provide the closed-form formulas for both σ^2 and σ_0^2 in the supplementary section A, and we describe the overall learning process in the Appendix, Algorithm 1.

Choice of \mathcal{G} For clarity, suppose that $g(\cdot, \cdot)$ belong to a family of distributions \mathcal{G} that have the following form:

$$g(\mathbf{d}_j, \theta) = \sum_{m=0}^M \pi_m(\mathbf{d}_j, \theta) g_m \quad (12)$$

$$\pi(\mathbf{d}_j, \theta) = (\pi_0(\mathbf{d}_j, \theta), \dots, \pi_M(\mathbf{d}_j, \theta)) \quad (13)$$

where g_m are fixed known distributions (e.g., $g_0 = \delta_0$ and $g_m = \mathcal{N}(0, \sigma_m^2)$ with $\sigma_m^2 < \sigma_{m+1}^2$ for all $m > 0$). Then $\pi(\cdot, \theta)$ is a neural network that takes side information \mathbf{d}_j as input and outputs a vector of probabilities $(\pi_0(\mathbf{d}_j, \theta), \dots, \pi_M(\mathbf{d}_j, \theta))$ that sum to 1 (e.g., using a softmax function). Under this model, the loss for θ has the following simple form:

$$\hat{\theta} = \arg \max_{\theta} \sum_{j=1}^P \log \sum_{m=0}^M \pi_m(\mathbf{d}_j, \theta) L_{jm} \quad (14)$$

where L_{jm} is defined as:

$$L_{jm} = \int p(\bar{\beta}_j | b_j) g_m(b_j) db_j \quad (15)$$

This represents the marginal likelihood of $\bar{\beta}_j$ under mixture component m . For Gaussian mixture components $g_m = \mathcal{N}(0, \sigma_m^2)$, we have:

$$L_{jm} = \mathcal{N}(\hat{\beta}_j; 0, \sigma_0^2 + \sigma_m^2) \quad (16)$$

These integrals often cannot be computed analytically for other priors and error models. However, (L_{jm}) are simple one-dimensional integrals that are fast to approximate. It is straightforward to extend this model to use more complex distribution mixtures such as Mixture Density Networks Bishop [1994] or Graph Mixture Density Networks Errica et al. [2021] (see section 4 for more details). More generally, $g(\cdot, \cdot)$ can be any probabilistic model (e.g., Gaussian Process, but potentially more complex models) for which the loss in 11 can be evaluated and the posterior $p(b_j | \bar{\beta}_j, \mathbf{d}_i, \sigma_0^2) \propto \mathcal{N}(\bar{\beta}_j; b_j, \sigma_0^2)g(b_i; \mathbf{d}_i, \hat{\theta})$ can be computed. For computational efficiency, it is useful that both of these steps can be evaluated via closed-form formulas. Note that when g does not depend on the covariate, then step 2) in the coordinate ascent described above corresponds to an empirical Bayes normal mean problem (EBNM; see Willwerscheid et al. [2024] for an overview, and [Robbins, 1956, Efron, 2019, Stephens, 2017] for classical statistical papers on this topic). In this case, fitting g as in 12 with fixed $g_m(\cdot)$ distributions corresponds to estimating the mixture proportions for the different mixture components $g_m(\cdot)$. Using fixed distributions is particularly practical as it allows efficient estimation of the mixture components (π_0, \dots, π_M) via sequential quadratic programming, which is often achieved in sub-linear time (in terms of p), see Kim et al. [2019].

3.2.1 On the Update for β

A careful reader will notice that the update for β can actually be solved exactly, without using an approximate posterior as in 7. Split VEB leads to an update for β that corresponds to a Bayesian ridge regression $\mathbf{y} | \mathbf{X}, \beta, \sigma^2 \sim N(\mathbf{X}\beta, \sigma^2)$ with a prior on $\beta \sim N(\mathbf{b}, \sigma_0^2 I_p)$. The posterior of β has a well-known closed form [Hoerl and Kennard, 1970]. However, computing this posterior requires inverting a matrix, resulting in $O(np^2 + p^3)$ operations to compute the exact posterior (or $O(n^2p + n^3)$ operations using the dual form, via Woodbury formula [Saunders et al., 1998]). Because of conjugacy and the assumption that the columns of \mathbf{X} are centered and scaled, the update at iteration $t + 1$ for β_j under 7 is given by $\beta_j^{t+1} = \omega \mathbf{x}_j^\top \bar{\mathbf{r}}_j^{t+1} + (1 - \omega) \bar{b}_j^t$. Here, $\bar{\mathbf{r}}_j^{t+1}$ is the expected residual at iteration $t + 1$ as defined in 9, \bar{b}_j^t is the posterior mean of b_j under 7 at iteration t , and $\mathbf{x}_j^\top \bar{\mathbf{r}}_j$ corresponds to the maximum likelihood estimate (MLE) of the effect of \mathbf{x}_j on $\bar{\mathbf{r}}_j^{t+1}$ due to scaling. The term ω is defined as $\omega = \frac{(n-1)\sigma_0^2}{\sigma^2 + (n-1)\sigma_0^2}$ as due to scaling $\mathbf{x}_j^\top \mathbf{x}_j = n - 1$. Therefore, each update for a β_j corresponds to a scalar product between two vectors, resulting in a coordinate ascent algorithm that has a complexity of $O(np)$, which is significantly smaller than $O(n^2p + n^3)$ or $O(np^2 + p^3)$.

3.2.2 An autoregressive update for g with auto-adaptive dampening

Given that in practice both σ^2 and σ_0^2 are being updated (see steps 3a and 3b in the coordinate ascent algorithm above), the resulting updates for g and q_b correspond to fitting a series of autoregressive covariate-moderated empirical Bayes normal mean problems (cEBNM) that have the following form:

$$\omega_t \hat{\beta}_{jMLE}^{t+1} + (1 - \omega_t) \bar{b}_j^t \sim N(b_j^{t+1}, \sigma_{0,t}^2), \quad (17)$$

$$b_j^{t+1} \sim g(\mathbf{d}_j, \boldsymbol{\theta}^{t+1}). \quad (18)$$

Here, $\omega_t = \frac{(n-1)\sigma_{0t}^2}{\sigma_t^2 + (n-1)\sigma_{0t}^2}$, where σ_{0t} is the value of σ_0^2 at iteration t (the same goes for σ_t^2). Equation 17 arises from basic Bayesian computation, yet it leads to an update that is simple to interpret. At each update for g and q_b , the model uses a proportion ω_t of novel evidence while retaining $1 - \omega_t$ of the previous update. Given that σ_t^2 and σ_{0t}^2 are maximized by Nash's ELBO, the parameter ω_t can be viewed as a data-driven dampening parameter for learning g and q_b .

3.3 Comparison and Connection with mr.ash

Our work is closely related to the multiple regression with adaptive shrinkage (mr.ash) proposed by Kim et al. [2024], but it differs in two key aspects. The most notable difference is that mr.ash cannot handle side information. A more technical yet important difference is our learning algorithm. Kim et al. [2024] use a standard CAVI for fitting VEB approximation of mr.ash, which results in a coordinate ascent algorithm that requires updating the prior g whenever updating q_{b_j} . Thus mr. ash's update for g corresponds to an M-step [Dempster et al., 1977]. Because the posterior and the prior learning steps are not decoupled in the mr.ash variational formulation, the resulting CAVI requires updating the prior g , p times per CAVI update. Split VEB allows decoupling these two problems,

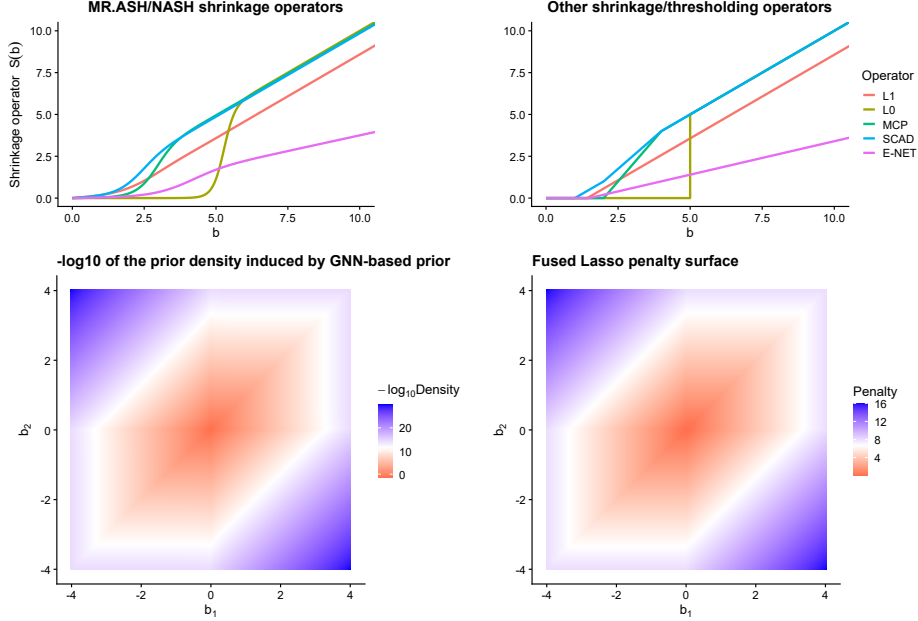


Figure 1: Upper panel: Adaptation of Figure 1 from Kim et al. [2024], showcasing that posterior mean shrinkage operators (left panel) for different choices of $\sigma_1^2, \dots, \sigma_M^2$ and π_0, \dots, π_M can mimic the shrinkage operators from some commonly used penalties (right-hand panel). Bottom panel left: Illustration of how Nash can mimic fused Lasso when used with a graph neural net prior-based. The left image presents the induced prior density from equation 23, allowing Nash to mimic the fused Lasso (using $s_1 = 0.45$ and $s_2 = 0.15$). Bottom right panel, penalty surface of the fused Lasso (i.e., $|b_1 + b_2| + |b_1 - b_2|$).

leading to a coordinate ascent for Nash that is notably more efficient as it only requires updating the prior g once per coordinate ascent update. While this nuance may appear subtle at first, it turns out to be crucial when side information is present. Using split VEB allows fitting Nash with a single update of the neural net parameters $\theta (g(\cdot, \theta))$ per coordinate ascent iteration. In contrast, adapting mr.ash would require updating the neural net p times per CAVI update, which is not practical when p is large.

$$\text{mr.ash} \qquad \qquad \qquad \text{Nash, without side information} \qquad \qquad (19)$$

$$\mathbf{y} | \mathbf{X}, \mathbf{b}, \sigma^2 \sim N(\mathbf{X}\mathbf{b}, \sigma^2) \qquad \mathbf{y} | \mathbf{X}, \boldsymbol{\beta}, \sigma^2 \sim N(\mathbf{X}\boldsymbol{\beta}, \sigma^2) \qquad (20)$$

$$b_j \sim g \qquad \qquad \qquad \beta_j \sim N(b_j, \sigma_0^2) \qquad (21)$$

$$b_j \sim g \qquad \qquad \qquad b_j \sim g \qquad (22)$$

These two works are related, as fitting Nash with split VEB when no side information is provided corresponds to optimizing a lower bound of mr. ash’s Evidence Lower Bound (ELBO), when using $g \in \mathcal{G}$ from the same family of distributions when fitting both models (see section B for a formal proof).

4 Connection to Penalized Linear Regression and Beyond

Kim et al. [2024] showed that mr.ash (and therefore Nash) can be viewed as a penalized linear regression (PLR) problem. When using an adaptive shrinkage prior (ash, [Stephens, 2017]) of the form $g = \pi_0 \delta_0 + \sum_{m=1}^M \pi_m N(0, \sigma_m^2)$, different choices of (π_0, \dots, π_M) corresponding to different penalties such as Ridge regression [Hoerl and Kennard, 1970], L0Learn [Hazimeh et al., 2023], Lasso [Tibshirani, 1996], Elastic Net [Zou and Hastie, 2005], the smoothly clipped absolute deviation (SCAD) penalty, and the minimax concave penalty (MCP) [Breheny and Huang, 2011]. The advantage

of mr.ash and Nash is that the user doesn't need to specify the penalty, as the model learns the mixture $(\hat{\pi}_0, \dots, \hat{\pi}_M)$ that best fits the data via EB. [Kim et al., 2024] proposed the concept of a shrinkage operator to properly establish the connection between EB multiple linear regression and PLR, which we depict in figure 1. We further build on this idea by suggesting that some parameterizations of Nash (detailed below) can be viewed as extensions to previous PLR methods with side information.

Group-Based and Hierarchical Penalty Several approaches have been developed to modulate the penalty based on groups or hierarchical structures of the data. Examples include the Group Lasso [Yuan and Lin, 2006], which uses a penalty of the form $\lambda_1 \|\mathbf{b}\|_1 + \lambda_2 \sum_{k \in \mathcal{K}} \sqrt{d_k} \|\mathbf{b}_k\|_2$, and the IPF-Lasso Boulesteix et al. [2017] with a penalty of the form $\lambda \sum_{k \in \mathcal{K}} \sum_{j \in k} \omega_k |b_j|$, where \mathcal{K} corresponds to the different groups or clusters. These cases are easily handled by Nash, as they simply correspond to fitting an ash prior per group/cluster/category. This is achieved using a prior of the form $g_k(\cdot) = \pi_{0k} \delta_0 + \sum_{m=1}^M \pi_{mk} N(0, \sigma_m^2)$ for each k . In other words the side information \mathbf{d}_j for the covariate \mathbf{x}_j is a vector of length \mathcal{K} with binary entries, where the k^{th} entry of \mathbf{d}_j is set to 1 if covariate j belongs to group k . Thus, the model $\pi : \mathbf{d}_j \rightarrow (\pi_0(\mathbf{d}_j), \dots, \pi_M(\mathbf{d}_j))$ is a multinomial regression that is straightforward to fit using standard machine learning routines. Unlike the Group Lasso or the IPF-Lasso, Nash can naturally fit different penalty types to different groups (e.g., fitting an L_1 like penalty on group 1 and fitting an L_2 like penalty on group 2).

Fused Lasso and Graph-Based Penalty The Fused Lasso [Tibshirani et al., 2005] aims to balance sparsity and smoothness covariates using a penalty of the for $\sum_{j=1}^p |b_j| \leq s_1$ and $\sum_{j=2}^p |b_j - b_{j-1}| \leq s_2$. Bayesian versions Casella et al. [2010], Betancourt et al. [2017] have been proposed. We extend these with graph neural networks (GNNs) to handle more complex dependencies. Classical Bayesian Fused Lasso Casella et al. [2010] can be reframed using a trivial graphical neural networks (GNN) [Kipf and Welling, 2017]. Here, $\mathbf{d}_j = \mathbf{d}_j^{t+1}$ is the graph (a line in the Fused Lasso case) with nodes storing $\beta_{j,MLE}^{t+1}$ and \bar{b}_j^t . As the model converges, $\bar{b}_{j+1}^t \approx \bar{b}_{j+1}^{t+1}$, aligning with classic formulations. We propose the EB Fused Lasso formulation:

$$g^{\text{fused}}(\mathbf{d}_j) = zL(0, s_1)L(l(\mathbf{d}_j), s_2)L(r(\mathbf{d}_j), s_2) \quad (23)$$

Here, $L(\mu, s_0)$ is a Laplace distribution centered at μ with scale s_0 , and z is a normalization constant. Functions $r(\mathbf{d}_j) = \bar{b}_{j-1}^t$ and $l(\mathbf{d}_j) = \bar{b}_{j+1}^t$ are trivial GNNs, allowing different strengths for previous and next values. Posterior moments for b_j can be approximated via Gauss-Hermite quadrature. Hyperparameters (s_1, s_2) are learned by maximizing the marginal log likelihood.

For an arbitrary graph, model 23 becomes computationally challenging as computing the posterior under a product of $k > 3$ Laplace distributions, as it quickly becomes computationally demanding to approximate. We propose **a generalized EB Fused Lasso** :

$$g^{\text{fused}}(\mathbf{d}_j) = zL(0, s_1)L(v_1(\mathbf{d}_j), s_2(\mathbf{d}_j)) \quad (24)$$

Here, $v_1(\mathbf{d}_j), (\mathbf{d}_j)$ is the output of a GNN output controlling b_j 's smoothness with respect to the graph structure. This simplifies normalization computation and integral approximation as it only uses two Laplace distributions.

Note that different variations of the Fused Lasso have been proposed, such as the Sparse Regression Incorporating Graphical Structure Among Predictors (SRIG) Yu et al. [2016] or the Graph-Guided Fused Lasso (GGFL) Chen et al. [2010]. The SRIG and GGFL penalties can also be mimicked by adapting the prior 24 using Normal instead of Laplace.

Beyond Regularization We also provide an implementation of Nash that uses penalties based on Mixture Density Networks (MDN) [Bishop, 1994] and Graph Mixture Density Networks (GMDN) [Errica et al., 2021]. The formulation is as follows:

$$g(j, \boldsymbol{\theta}) = \pi_0(\mathbf{d}_j) \delta_0 + \sum_k \pi_k(\mathbf{d}_j) N(\mu_k(\mathbf{d}_j), \sigma_k^2(\mathbf{d}_j)) \quad (25)$$

Here, $(\pi_k(\mathbf{d}_j)), (\mu_k(\mathbf{d}_j)), (\sigma_k^2(\mathbf{d}_j))$ are the outputs of the (graph) MDN, as described in Bishop [1994] and in Errica et al. [2021]. These parameterizations allow the model to actually push the values of b_j away from 0. Enabling Nash to be used as a "self-supervised" biased regression where the bias (here $\mu_k(\mathbf{d}_j)$) is automatically learned from the data.

5 Numerical Experiment

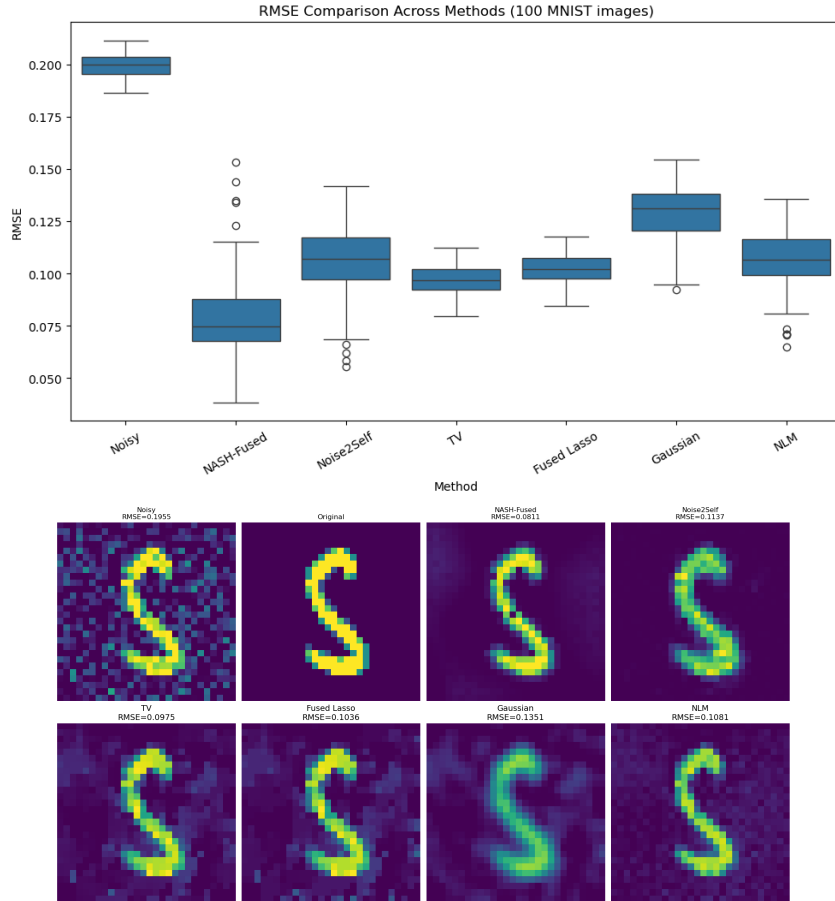


Figure 2: Top panel: performances of the different approaches for denoising MNIST image in terms of RMSE. Bottom panel: sample from the experiment showcasing the performance of Nash-fused.

We evaluate Nash prediction performance on 4 real data sets that have side information. In each of these datasets, we also benchmark the performance of mr.ash, Lasso, the elastic net (Enet) with $\alpha = 0.5$, ridge regression, and when the data display group/hierarchical side information, we also benchmark the ipf Lasso. We benchmark 2 versions of Nash: i) Nash without side information and ii) Nash-mdn equation 25. We also benchmark the performance of xgboost [Chen and Guestrin, 2016], and multi-layer perceptron (MLP) with L2 regularization.

We selected a range of real datasets that spans from small data set and with a limited number of covariates (e.g. Air Passenger data) to larger data set scale such as epigenetic age prediction with nearly 500,000 predictors. We detail these datasets and the preprocessing in B.2. In most of our experiment we proceed as follow, we remove at random 20% of the data for testing purposes and run the different on the remaining data and evaluate the performance of each methods in terms of rmse.

- **SNP500**: we used daily return from of the **AAPL** symbols from SNP500 using other assets daily return. For each asset used in the predictor, we obtained the type of industry in which this asset is part of (e.g., Technology, Communication Services, Healthcare, Equity Funds) and used it as side information.
- **Airpassenger**: we added noise to the Airpassenger data set and used the measurement time point as side information.

- **GSE40279**: we used methylation data from individuals measurement ($p = 489,503$) to predict the age of the subject [Bohlin et al., 2016, Horvath and Raj, 2018]. We use methylation probe annotation as side information.
- **TCGA**: we predict individual normalized *BRCA1* gene expression (an important gene in breast cancer) expression level using the other genes. We use gene pathways from KEGG pathway as side information.

Method	SNP500	Airpassenger	GSE40279	TCGA
Dimension ($n \times p$)	235 \times 85	144 \times 144	679 \times 489,503	1,212 \times 18,300
Side info	group	time	probe type	pathway
Ridge	0.070 (0.065; 0.076)	33.0 (31.0; 35.0)	7.21 (6.83; 7.58)	0.536 (0.472; 0.599)
Enet	0.071 (0.066; 0.078)	30.2 (29.5; 30.9)	5.28 (5.02; 5.56)	0.466 (0.411; 0.522)
Lasso	0.093 (0.087; 0.100)	49.2 (48.7; 49.7)	5.39 (5.08; 5.71)	0.465 (0.412; 0.518)
mr.ash	0.082 (0.076; 0.088)	20.2 (19.1; 21.3)	5.25 (5.01; 5.71)	0.449 (0.405; 0.493)
XGBoost	0.062 (0.053; 0.069)	18.2 (17.2; 19.1)	6.17 (5.83; 6.52)	0.549 (0.494; 0.604)
MLP	0.441 (0.361; 0.521)	59.5 (58.3; 60.8)	13.62 (13.08; 14.15)	0.457 (0.349; 0.566)
ipf-Lasso	0.066 (0.060; 0.072)	NA	5.06 (4.81; 5.33)	0.443 (0.393; 0.473)
Nash.no.cov	0.084 (0.079; 0.089)	19.7 (18.6; 20.7)	5.27 (5.01; 5.53)	0.457 (0.412; 0.504)
Nash.mdn	0.058 (0.053; 0.0643)	17.7 (17.1; 18.2)	5.12 (4.77; 5.47)	0.435 (0.387; 0.483)

Table 1: Comparison of methods across datasets using RMSE. Parentheses denote 95% confidence intervals based on Gaussian approximations. ipf-Lasso cannot handle time as side information, so we put NA for the Airpassenger experiment.

5.1 Denoising MNIST Images

We evaluate the performance of Nash-fused 23 using a simple 2-layer message passing GNN to remove Gaussian noise in images compared to methods for image denoising that only use a **single image** (as opposed to models trained on other images like diffusion model), such as fused-lasso [Tibshirani et al., 2005], Total Variation (TV) Denoising Chambolle [2004], Non-Local Means (NLM) [Buades et al., 2005], Gaussian Filtering [Gonzalez and Woods, 2002], Median Filtering [Huang et al., 1979], and Noise2Self [Batson and Royer, 2019] of denoising noisy grayscale images from the MNIST dataset. Nash-fused was run treating each image as a 2D grid graph, where each pixel is a node connected to its 4-nearest neighbors, and Noise2Self was run using a convolutional neural net, which is substantially slower than Nash-fused. The true signal is the clean MNIST digit image scaled to $[0,1]$, and additive Gaussian noise with as standard deviation of $\sigma = 0.2$ was applied to produce the observed noisy image. The experiment is repeated over 100 randomly selected MNIST images. For each method, we report the root mean squared error (RMSE) between the denoised image and the ground truth. Results are summarized as boxplots in Figure 2. We have some additional examples of denoised images using Nash-fused in the Appendix (see figure3-9)

6 Discussion

We proposed Nash, a novel high-dimensional regression framework that integrates covariate-specific side information into the estimation process using neural networks. Nash adaptively learns structured penalties in a nonparametric fashion, enabling flexible regularization without the need for cross-validation. Our method generalizes and extends existing approaches that incorporate side information, offering a unified and more expressive framework. We also proposed a new learning algorithm, split variational empirical Bayes (split VEB), which decouples prior learning from posterior inference, allowing for efficient and scalable optimization. This algorithm naturally connects to and simplifies a recently proposed variational Empirical Bayes approach [Kim et al., 2024], while supporting far richer prior families, including those parameterized by deep neural networks.

To our knowledge, Nash is the first regression method that models the prior distribution over regression effects as a direct function of side information, enabling automatic, data-driven regularization across diverse structures such as groups, time, and graphs. Through extensive experiments on real and synthetic datasets, we demonstrated that Nash consistently performs competitively and can outperform existing methods tailored to handle a **specific** type of side information.

References

- Arthur E. Hoerl and Robert W. Kennard. Ridge Regression: Biased Estimation for Nonorthogonal Problems. *Technometrics*, 12(1):55–67, 1970. ISSN 0040-1706. doi: 10.2307/1267351. URL <https://www.jstor.org/stable/1267351>. Publisher: [Taylor & Francis, Ltd., American Statistical Association, American Society for Quality].
- Robert Tibshirani. Regression Shrinkage and Selection Via the Lasso. *Journal of the Royal Statistical Society: Series B (Methodological)*, 58(1):267–288, 1996. ISSN 2517-6161. doi: 10.1111/j.2517-6161.1996.tb02080.x. URL <https://rss.onlinelibrary.wiley.com/doi/abs/10.1111/j.2517-6161.1996.tb02080.x>.
- Hui Zou and Trevor Hastie. Regularization and Variable Selection Via the Elastic Net. *Journal of the Royal Statistical Society Series B: Statistical Methodology*, 67(2):301–320, April 2005. ISSN 1369-7412, 1467-9868. doi: 10.1111/j.1467-9868.2005.00503.x. URL <https://academic.oup.com/jrsssb/article/67/2/301/7109482>.
- Steve Horvath and Kenneth Raj. DNA methylation-based biomarkers and the epigenetic clock theory of ageing. *Nature Reviews Genetics*, 19(6):371, June 2018. ISSN 1471-0064. doi: 10.1038/s41576-018-0004-3. URL <https://www.nature.com/articles/s41576-018-0004-3>.
- J. Bohlin, S. E. Håberg, P. Magnus, S. E. Reese, H. K. Gjessing, M. C. Magnus, C. L. Parr, C. M. Page, S. J. London, and W. Nystad. Prediction of gestational age based on genome-wide differentially methylated regions. *Genome Biology*, 17(1):207, October 2016. ISSN 1474-760X. doi: 10.1186/s13059-016-1063-4. URL <https://doi.org/10.1186/s13059-016-1063-4>.
- Kristine L. Haftorn, Yunsung Lee, William R. P. Denault, Christian M. Page, Haakon E. Nustad, Robert Lyle, Håkon K. Gjessing, Anni Malmberg, Maria C. Magnus, Øyvind Næss, Darina Czamara, Katri Räikkönen, Jari Lahti, Per Magnus, Siri E. Håberg, Astanand Jugessur, and Jon Bohlin. An EPIC predictor of gestational age and its application to newborns conceived by assisted reproductive technologies. *Clinical Epigenetics*, 13(1):82, April 2021. ISSN 1868-7083. doi: 10.1186/s13148-021-01055-z. URL <https://doi.org/10.1186/s13148-021-01055-z>.
- Sander Devriendt, Katrien Antonio, Tom Reynkens, and Roel Verbelen. Sparse Regression with Multi-type Regularized Feature Modeling. *Insurance: Mathematics and Economics*, 96:248–261, January 2021. ISSN 01676687. doi: 10.1016/j.insmatheco.2020.11.010. URL <http://arxiv.org/abs/1810.03136>. arXiv:1810.03136 [stat].
- Anne-Laure Boulesteix, Riccardo De Bin, Xiaoyu Jiang, and Mathias Fuchs. IPF-LASSO: Integrative L1-Penalized Regression with Penalty Factors for Prediction Based on Multi-Omics Data. *Computational and Mathematical Methods in Medicine*, 2017:7691937, 2017. ISSN 1748-6718. doi: 10.1155/2017/7691937.
- Robert Tibshirani, Michael Saunders, Saharon Rosset, Ji Zhu, and Keith Knight. Sparsity and smoothness via the fused lasso. *Journal of the Royal Statistical Society: Series B (Statistical Methodology)*, 67(1):91–108, 2005. ISSN 1467-9868. doi: 10.1111/j.1467-9868.2005.00490.x. URL <https://rss.onlinelibrary.wiley.com/doi/abs/10.1111/j.1467-9868.2005.00490.x>.
- Ming Yuan and Yi Lin. Model selection and estimation in regression with grouped variables. *Journal of the Royal Statistical Society: Series B (Statistical Methodology)*, 68(1):49–67, 2006. ISSN 1467-9868. doi: 10.1111/j.1467-9868.2005.00532.x. URL <https://onlinelibrary.wiley.com/doi/abs/10.1111/j.1467-9868.2005.00532.x>. _eprint: <https://onlinelibrary.wiley.com/doi/pdf/10.1111/j.1467-9868.2005.00532.x>.
- Guan Yu, , and Yufeng Liu. Sparse Regression Incorporating Graphical Structure Among Predictors. *Journal of the American Statistical Association*, 111(514):707–720, April 2016. ISSN 0162-1459. doi: 10.1080/01621459.2015.1034319. URL <https://doi.org/10.1080/01621459.2015.1034319>. Publisher: ASA Website _eprint: <https://doi.org/10.1080/01621459.2015.1034319>.
- Dongyue Xie. *Empirical Bayes methods for count data*. PhD thesis, 2023.
- Youngseok Kim, Wei Wang, Peter Carbonetto, and Matthew Stephens. A flexible empirical Bayes approach to multiple linear regression and connections with penalized regression. *Journal of Machine Learning Research*, 25(185):1–59, 2024. ISSN 1533-7928. URL <http://jmlr.org/papers/v25/22-0953.html>.
- Tianqi Chen and Carlos Guestrin. XGBoost: A Scalable Tree Boosting System. In *Proceedings of the 22nd ACM SIGKDD International Conference on Knowledge Discovery and Data Mining*, pages

- 785–794, San Francisco California USA, August 2016. ACM. ISBN 978-1-4503-4232-2. doi: 10.1145/2939672.2939785. URL <https://dl.acm.org/doi/10.1145/2939672.2939785>.
- Jan Gertheiss and Gerhard Tutz. Sparse modeling of categorical explanatory variables. *The Annals of Applied Statistics*, 4(4):2150–2180, December 2010. ISSN 1932-6157, 1941-7330. doi: 10.1214/10-AOAS355. URL <https://projecteuclid.org/journals/annals-of-applied-statistics/volume-4/issue-4/Sparse-modeling-of-categorical-explanatory-variables/10.1214/10-AOAS355.full>. Publisher: Institute of Mathematical Statistics.
- Gerhard Tutz and Margret-Ruth Oelker. Modelling Clustered Heterogeneity: Fixed Effects, Random Effects and Mixtures. *International Statistical Review*, 85(2):204–227, 2017. ISSN 1751-5823. doi: 10.1111/insr.12161. URL <https://onlinelibrary.wiley.com/doi/abs/10.1111/insr.12161>. _eprint: <https://onlinelibrary.wiley.com/doi/pdf/10.1111/insr.12161>.
- Margret-Ruth Oelker and Gerhard Tutz. A uniform framework for the combination of penalties in generalized structured models. *Advances in Data Analysis and Classification*, 11(1):97–120, March 2017. ISSN 1862-5355. doi: 10.1007/s11634-015-0205-y. URL <https://doi.org/10.1007/s11634-015-0205-y>.
- Ryan J. Tibshirani and Jonathan Taylor. The solution path of the generalized lasso. *The Annals of Statistics*, 39(3):1335–1371, June 2011. ISSN 0090-5364, 2168-8966. doi: 10.1214/11-AOS878. URL <https://projecteuclid.org/journals/annals-of-statistics/volume-39/issue-3/The-solution-path-of-the-generalized-lasso/10.1214/11-AOS878.full>. Publisher: Institute of Mathematical Statistics.
- D. I. Okoh, G. K. Seemala, A. B. Rabi, J. Uwamahoro, J. B. Habarulema, and M. Aggarwal. A Hybrid Regression-Neural Network (HR-NN) Method for Forecasting the Solar Activity. *Space Weather*, 16(9):1424–1436, 2018. ISSN 1542-7390. doi: 10.1029/2018SW001907. URL <https://onlinelibrary.wiley.com/doi/abs/10.1029/2018SW001907>. _eprint: <https://onlinelibrary.wiley.com/doi/pdf/10.1029/2018SW001907>.
- Eric Nalisnick, Akihiro Matsukawa, Yee Whye Teh, Dilan Gorur, and Balaji Lakshminarayanan. Hybrid Models with Deep and Invertible Features. In *Proceedings of the 36th International Conference on Machine Learning*, pages 4723–4732. PMLR, May 2019. URL <https://proceedings.mlr.press/v97/nalisnick19b.html>. ISSN: 2640-3498.
- Ismael Lemhadri, Feng Ruan, Louis Abraham, and Robert Tibshirani. LassoNet: A Neural Network with Feature Sparsity. *Journal of Machine Learning Research*, 22(127):1–29, 2021. ISSN 1533-7928. URL <http://jmlr.org/papers/v22/20-848.html>.
- Nicholas G. Polson, James G. Scott, and Brandon T. Willard. Proximal Algorithms in Statistics and Machine Learning. *Statistical Science*, 30(4):559–581, November 2015. ISSN 0883-4237, 2168-8745. doi: 10.1214/15-STS530. URL <https://projecteuclid.org/journals/statistical-science/volume-30/issue-4/Proximal-Algorithms-in-Statistics-and-Machine-Learning/10.1214/15-STS530.full>. Publisher: Institute of Mathematical Statistics.
- Hugh Chipman, Edward I. George, and Robert E. McCulloch. The Practical Implementation of Bayesian Model Selection. In *Model Selection*, volume 38 of *IMS Lecture Notes – Monograph Series*, pages 65–116. Institute of Mathematical Statistics, 2001.
- Wei Wang and Matthew Stephens. Empirical Bayes Matrix Factorization. *Journal of Machine Learning Research*, 22(120):1–40, 2021. ISSN 1533-7928. URL <http://jmlr.org/papers/v22/20-589.html>.
- Christopher M. Bishop. Mixture Density Networks. Technical Report NCRG/94/004, Aston University, Birmingham, UK, 1994. URL https://publications.aston.ac.uk/id/eprint/373/1/NCRG_94_004.pdf.
- Federico Errica, Davide Bacciu, and Alessio Micheli. Graph Mixture Density Networks. In *Proceedings of the 38th International Conference on Machine Learning*, volume 139 of *Proceedings of Machine Learning Research*, pages 3025–3035. PMLR, 2021. URL <https://proceedings.mlr.press/v139/errica21a.html>.

- Jason Willwerscheid, Peter Carbonetto, and Matthew Stephens. ebnm: An R Package for Solving the Empirical Bayes Normal Means Problem Using a Variety of Prior Families, March 2024. URL <http://arxiv.org/abs/2110.00152>. arXiv:2110.00152 [stat].
- Herbert Robbins. An Empirical Bayes Approach to Statistics. *Proceedings of the Third Berkeley Symposium on Mathematical Statistics and Probability, Volume 1: Contributions to the Theory of Statistics*, 3.1:157–164, January 1956. URL <https://projecteuclid.org/ebooks/berkeley-symposium-on-mathematical-statistics-and-probability/Proceedings-of-the-Third-Berkeley-Symposium-on-Mathematical-Statistics-and-probability/chapter/An-Empirical-Bayes-Approach-to-Statistics/bsmsp/1200501653>. Publisher: University of California Press.
- Bradley Efron. Bayes, Oracle Bayes and Empirical Bayes. *Statistical Science*, 34(2): 177–201, May 2019. ISSN 0883-4237, 2168-8745. doi: 10.1214/18-STS674. URL <https://projecteuclid.org/journals/statistical-science/volume-34/issue-2/Bayes-Oracle-Bayes-and-Empirical-Bayes/10.1214/18-STS674.full>. Publisher: Institute of Mathematical Statistics.
- Matthew Stephens. False discovery rates: a new deal. *Biostatistics*, 18(2):275–294, April 2017. ISSN 1465-4644. doi: 10.1093/biostatistics/kxw041. URL <https://academic.oup.com/biostatistics/article/18/2/275/2557030>.
- Youngseok Kim, Peter Carbonetto, Matthew Stephens, and Mihai Anitescu. A Fast Algorithm for Maximum Likelihood Estimation of Mixture Proportions Using Sequential Quadratic Programming. *Journal of Computational and Graphical Statistics*, 0(0):1–13, November 2019. ISSN 1061-8600. doi: 10.1080/10618600.2019.1689985. URL <https://doi.org/10.1080/10618600.2019.1689985>.
- Craig Saunders, Alexander Gammernan, and Volodya Vovk. Ridge Regression Learning Algorithm in Dual Variables. In *Proceedings of the 15th International Conference on Machine Learning (ICML)*, pages 515–521. Morgan Kaufmann, 1998. URL https://eprints.soton.ac.uk/258942/1/Dualrr_ICML98.pdf.
- A. P. Dempster, N. M. Laird, and D. B. Rubin. Maximum Likelihood from Incomplete Data via the EM Algorithm. *Journal of the Royal Statistical Society. Series B (Methodological)*, 39(1):1–38, 1977. ISSN 0035-9246. URL <https://www.jstor.org/stable/2984875>.
- Hussein Hazimeh, Rahul Mazumder, and Tim Nonet. L0Learn: A Scalable Package for Sparse Learning using L0 Regularization. *Journal of Machine Learning Research*, 24(205):1–8, 2023. ISSN 1533-7928. URL <http://jmlr.org/papers/v24/22-0189.html>.
- Patrick Breheny and Jian Huang. Coordinate descent algorithms for nonconvex penalized regression, with applications to biological feature selection. *The Annals of Applied Statistics*, 5(1):232–253, March 2011. ISSN 1932-6157, 1941-7330. doi: 10.1214/10-AOAS388. URL <https://projecteuclid.org/journals/annals-of-applied-statistics/volume-5/issue-1/Coordinate-descent-algorithms-for-nonconvex-penalized-regression-with-applications-to/10.1214/10-AOAS388.full>. Publisher: Institute of Mathematical Statistics.
- George Casella, Malay Ghosh, Jeff Gill, and Minjung Kyung. Penalized regression, standard errors, and Bayesian lassos. *Bayesian Analysis*, 5(2):369–411, June 2010. ISSN 1936-0975, 1931-6690. doi: 10.1214/10-BA607. URL <https://projecteuclid.org/journals/bayesian-analysis/volume-5/issue-2/Penalized-regression-standard-errors-and-Bayesian-lassos/10.1214/10-BA607.full>. Publisher: International Society for Bayesian Analysis.
- Brenda Betancourt, Abel Rodríguez, and Naomi Boyd. Bayesian Fused Lasso Regression for Dynamic Binary Networks. *Journal of Computational and Graphical Statistics*, October 2017. ISSN 1061-8600. URL <https://www.tandfonline.com/doi/full/10.1080/10618600.2017.1341323>. Publisher: Taylor & Francis.
- Thomas N Kipf and Max Welling. SEMI-SUPERVISED CLASSIFICATION WITH GRAPH CONVOLUTIONAL NETWORKS. 2017.
- Xi Chen, Seyoung Kim, Qihang Lin, Jaime G. Carbonell, and Eric P. Xing. Graph-Structured Multi-task Regression and an Efficient Optimization Method for General Fused Lasso, May 2010. URL <http://arxiv.org/abs/1005.3579>. arXiv:1005.3579 [stat].

- Antonin Chambolle. An algorithm for total variation minimization and applications. *Journal of Mathematical Imaging and Vision*, 20(1-2):89–97, 2004. Publisher: Springer.
- A. Buades, B. Coll, and J.-M. Morel. A non-local algorithm for image denoising. In *2005 IEEE Computer Society Conference on Computer Vision and Pattern Recognition (CVPR'05)*, volume 2, pages 60–65 vol. 2, June 2005. doi: 10.1109/CVPR.2005.38. URL <https://ieeexplore.ieee.org/document/1467423>. ISSN: 1063-6919.
- Rafael C. Gonzalez and Richard E. Woods. *Digital Image Processing*. Prentice Hall, Upper Saddle River, NJ, USA, 2nd edition, 2002.
- T. Huang, G. Yang, and G. Tang. A fast two-dimensional median filtering algorithm. *IEEE Transactions on Acoustics, Speech, and Signal Processing*, 27(1):13–18, February 1979. ISSN 0096-3518. doi: 10.1109/TASSP.1979.1163188. URL <https://ieeexplore.ieee.org/document/1163188>.
- Joshua Batson and Laurent Royer. Noise2Self: Blind Denoising by Self-Supervision. In Kamalika Chaudhuri and Ruslan Salakhutdinov, editors, *Proceedings of the 36th International Conference on Machine Learning*, volume 97 of *Proceedings of Machine Learning Research*, pages 524–533. PMLR, 2019.

A Detailed split VEB for the Nash model

The Nash model with side information can be written as:

$$\mathbf{y}|\mathbf{X}, \boldsymbol{\beta}, \sigma^2 \sim N(\mathbf{X}\boldsymbol{\beta}, \sigma^2) \quad (26)$$

$$\beta_j \sim N(b_j, \sigma_0^2) \quad (27)$$

$$b_j \sim g(\cdot; \mathbf{d}_j, \theta) \quad (28)$$

As noted in our manuscript we restrict our search to posterior of the form

$$q(\boldsymbol{\beta}, \mathbf{b}) = \prod_j^P q_{\beta_j}(\beta_j) q_{b_j}(b_j) \quad (29)$$

The overall evidence lower bound (ELBO) is

$$F(q_{\boldsymbol{\beta}}, q_{\mathbf{b}}, g; \sigma^2, \sigma_0^2)_{Nash} = \sum_i \mathbb{E} \log \frac{p(y_i | \mathbf{x}_i, \boldsymbol{\beta}, \sigma^2)}{q_{\boldsymbol{\beta}}(\boldsymbol{\beta})} + \sum_j \mathbb{E} \log p(\beta_j | b_j, \sigma_0^2) + \sum_j \mathbb{E} \log \frac{g(b_j; \mathbf{d}_j, \theta)}{q_{b_j}(b_j)} \quad (30)$$

Our coordinate-ascent algorithm iterates between the updating $q_{\boldsymbol{\beta}}$ and updating $(q_{\mathbf{b}}, g(\cdot; \cdot, \theta))$.

A.1 Update for q_{β_j}

Note that given that when $q_{\mathbf{b}}, g(\cdot; \cdot, \theta)$ are fixed then the objective for q_{β_j} , $j = 1, \dots, P$ is

$$F(q_{\beta_j}) = \mathbb{E} \log(p(\mathbf{y} | \mathbf{x}_j, \beta_j, \mathbf{X}_{-j}, \boldsymbol{\beta}_{-j}, \sigma^2)) + \mathbb{E} \log p(\beta_j | \bar{b}_j, \sigma_0^2) - \mathbb{E} \log q_{\beta_j} \quad (31)$$

$$= \mathbb{E} \log(p(\bar{\mathbf{r}}_j | \mathbf{x}_j, \beta_j, \sigma^2)) + \mathbb{E} \log p(\beta_j | \bar{b}_j, \sigma_0^2) - \mathbb{E} \log q_{\beta_j} \quad (32)$$

where $\bar{\mathbf{r}}_j = \mathbf{y} - \mathbf{X}_{-j} \bar{\boldsymbol{\beta}}_{-j}$, this is direct consequence of Proposition 1 of Kim et al. [2024]), so the and so $q_{\beta_j}^* = \text{max} F(q_{\beta_j})$ is given by computing the posterior of the following simple model

$$\bar{\mathbf{r}}_j = \mathbf{x}_j \beta_j + \varepsilon \quad (33)$$

$$\beta_j \sim \mathcal{N}(\bar{b}_j, \sigma_0^2) \quad (34)$$

$$\varepsilon \sim \mathcal{N}(0, \sigma^2) \quad (35)$$

By conjugacy, the posterior distribution of β_j has the following form $\beta_j | \bar{\mathbf{r}}_j, \mathbf{x}_j \sim \mathcal{N}(\bar{\beta}_j, s_j^2)$ with posterior variance $s_j^2 = \left(\frac{\mathbf{x}_j^t \mathbf{x}_j}{\sigma^2} + \frac{1}{\sigma_0^2} \right)^{-1}$ and posterior mean $\bar{\beta}_j = s_j^2 \left(\frac{\mathbf{x}_j^t \bar{\mathbf{r}}_j}{\sigma^2} + \frac{\bar{b}_j}{\sigma_0^2} \right)$. In practice given that the column of \mathbf{X} are centered $\mathbf{x}_j^t \mathbf{x}_j^t = n - 1$ for all $j = 1, \dots, p$.

A.2 Update for $q_{\mathbf{b}}$ and g

Given $q_{\boldsymbol{\beta}}$ and σ^2 , the objective function for $(q_{\mathbf{b}}, g(\cdot; \cdot, \theta))$ is

$$F(q_{\mathbf{b}}, g(\cdot; \cdot, \theta)) = \sum_j \mathbb{E} \log p(\bar{\beta}_j | b_j, \sigma_0^2) + \sum_j \mathbb{E} \log \frac{g(b_j; \mathbf{d}_j, \theta)}{q_{b_j}(b_j)} \quad (36)$$

This objective corresponds to a so-called (covariate)moderated normal mean problem (see [Stephens, 2017, Willwerscheid et al., 2024]) that we detail below

The cEBNM problem Given p observations $\bar{\beta}_j \in \mathbb{R}$ with known standard deviations $s_j^2 > 0$, $j = 1, \dots, p$, the normal means model [Stephens, 2017] is

$$\bar{\beta}_j \stackrel{\text{ind.}}{\sim} N(b_j, \sigma_0^2), \quad (37)$$

where the ‘‘true’’ means $b_j \in \mathbb{R}$ are unknown. We further assume that

$$b_j \stackrel{\text{i.i.d.}}{\sim} g \in \mathcal{G}, \quad (38)$$

where \mathcal{G} is some prespecified family of probability distributions. The empirical Bayes (EB) approach to fitting this model exploits the fact that the noisy observations $\bar{\beta}_j$, contain not only information about the underlying means b_j but also about how the means are collectively distributed (i.e., g). EB approaches ‘‘borrow information’’ across the observations to estimate g , typically by maximizing the marginal log-likelihood. The unknown means b_j are generally estimated by their posterior mean.

We adapt EBNM to a covariate moderated setting (covariate moderated EBNM, cEBNM), where we allow the prior for the j -th unknown mean to depend on additional data \mathbf{d}_j ,

$$b_j \stackrel{\text{ind.}}{\sim} g(\mathbf{d}_j, \boldsymbol{\theta}) \in \mathcal{G}, \quad (39)$$

so that each combination of $\boldsymbol{\theta}$ and \mathbf{d}_j maps to an element of \mathcal{G} . We refer to this modified EBNM model as ‘‘covariate-moderated EBNM’’ (cEBNM).

Solving the cEBNM problem, therefore, involves two key computations:

1. Estimate the model parameters. Compute

$$\hat{\boldsymbol{\theta}} := \underset{\boldsymbol{\theta} \in \mathbf{R}^m}{\operatorname{argmax}} \mathcal{L}(\boldsymbol{\theta}), \quad (40)$$

where $\mathcal{L}(\boldsymbol{\theta})$ denotes the marginal likelihood,

$$\mathcal{L}(\boldsymbol{\theta}) := p(\bar{\boldsymbol{\beta}} \mid \mathbf{s}, \boldsymbol{\theta}, \mathbf{D}) = \prod_{j=1}^p \int \mathcal{N}(\bar{\beta}_j; b_j, \sigma_0^2) g(b_j; \mathbf{d}_j, \boldsymbol{\theta}) db_j, \quad (41)$$

in which $\bar{\boldsymbol{\beta}} = (\bar{\beta}_1, \dots, \bar{\beta}_p)$, $\mathbf{s} = (s_1, \dots, s_n)$, \mathbf{D} is a matrix storing $\mathbf{d}_1, \dots, \mathbf{d}_p$, and $\mathcal{N}(\bar{\beta}_j; b_j, \sigma_0^2)$ denotes the density of $\mathcal{N}(b_j, \sigma_0^2)$ at $\bar{\beta}_j$, and $g(b_j; \mathbf{d}_j, \boldsymbol{\theta})$ denotes the density of $g(\mathbf{d}_j, \boldsymbol{\theta})$ at b_j .

2. Compute posterior summaries. Compute summaries from the posterior distributions, such as the posterior means $\bar{b}_j := \mathbb{E}[b_j \mid \bar{\beta}_j, s_j, \hat{\boldsymbol{\theta}}, \mathbf{D}]$, using the estimated prior,

$$p(b_j \mid \bar{\beta}_j, s_j, \hat{\boldsymbol{\theta}}, \mathbf{D}) \propto \mathcal{N}(\hat{\beta}_j; b_j, \sigma_0^2) g(b_j; \mathbf{d}_j, \hat{\boldsymbol{\theta}}). \quad (42)$$

In summary, solving the cEBNM problem consists of finding a mapping from known quantities $(\bar{\boldsymbol{\beta}}, \mathbf{s}, \mathbf{D})$ to a tuple $(\hat{\boldsymbol{\theta}}, q)$, where each $(\mathbf{d}_j, \hat{\boldsymbol{\theta}})$ maps to an element $g(\mathbf{d}_j, \boldsymbol{\theta}) \in \mathcal{G}$, and q is the posterior distribution of the unobserved \mathbf{b} given $(\bar{\boldsymbol{\beta}}, \mathbf{s}, \mathbf{D})$. We denote this mapping as

$$\text{cEBNM}(\bar{\boldsymbol{\beta}}, \mathbf{s}, \mathbf{D}) = (\hat{\boldsymbol{\theta}}, q). \quad (43)$$

Any prior family is admissible under the cEBMF framework so long as 43 is computable.

A.3 update for σ and σ_0^2

The update for σ and σ_0^2 are obtained by simply maximizing the ELBO $F(q_{\boldsymbol{\beta}}, q_{\mathbf{b}}, g; \sigma^2, \sigma_0^2)_{\text{Nash}}$ with respect to σ and σ_0^2 , i.e;

$$(\sigma^2)^* = \underset{\sigma^2}{\operatorname{argmax}} F(q_{\boldsymbol{\beta}}, q_{\mathbf{b}}, g; \sigma^2, \sigma_0^2)_{\text{Nash}} \quad (44)$$

$$(\sigma_0^2)^* = \underset{\sigma_0^2}{\operatorname{argmax}} F(q_{\boldsymbol{\beta}}, q_{\mathbf{b}}, g; \sigma^2, \sigma_0^2)_{\text{Nash}} \quad (45)$$

It turns out that using results from [Wang and Stephens, 2021] and Kim et al. [2024] that the update for

$$\sigma^2 = \frac{\|\mathbf{y} - \mathbf{X}\boldsymbol{\beta}\| + \boldsymbol{\beta}^t(\boldsymbol{\beta}_{MLE} - \boldsymbol{\beta}) + \sigma^2 p}{n + p} \quad (46)$$

$$\sigma_0^2 = \frac{\|\mathbf{y} - \mathbf{X}\mathbf{b}\| + \mathbf{b}^t(\boldsymbol{\beta} - \mathbf{b}) + \sigma_0^2 p \left(1 - \frac{\sum_j \pi_0(\mathbf{d}_j)}{p}\right)}{n + p \left(1 - \frac{\sum_j \pi_0(\mathbf{d}_j)}{p}\right)} \quad (47)$$

$$(48)$$

Where $\boldsymbol{\beta}_{MLE}$ is the vector of $\mathbf{x}_j^t \bar{\mathbf{r}}_j$ as defined in the section A.1.

Algorithm 1 Algorithm for the split VEB coordinate ascent for Nash.

Require: Data $\mathbf{X} \in \mathbb{R}^{n \times p}$, $\mathbf{y} \in \mathbb{R}^n$; a model for $g(\cdot, \theta)$;

1: prior variances, $\sigma_1^2 < \dots < \sigma_K^2$, with $\sigma_1^2 = 0$; initial estimates $\boldsymbol{\beta}, \mathbf{b}, \boldsymbol{\pi}, \sigma^2$.

2: $t=0$

3: **repeat**

4: **for** $j = 1$ to p **do**

5: $\bar{\mathbf{r}}_j \leftarrow \bar{\mathbf{r}} + \mathbf{x}_j \bar{\boldsymbol{\beta}}_j^t$ ▷ disregard j th effect

6: $\tilde{\boldsymbol{\beta}}_j^{t+1} \leftarrow \mathbf{x}_j^T \bar{\mathbf{r}}_j$ ▷ OLS

7: $\bar{\boldsymbol{\beta}}_j^{t+1} \leftarrow \omega_t \tilde{\boldsymbol{\beta}}_j^{t+1} + (1 - \omega_t) \bar{b}_j^t$ ▷ Posterior mean Ridge

8: $\bar{\mathbf{r}} \leftarrow \bar{\mathbf{r}} - \mathbf{x}_j \bar{\boldsymbol{\beta}}_j^t$

9: **end for**

10: $\hat{\boldsymbol{\theta}} = \arg \max_{\boldsymbol{\theta}} \prod_{j=1}^p \int \mathcal{N}(\bar{\boldsymbol{\beta}}_j^{t+1}; b_j, \sigma_0^2) g(b_j; \mathbf{d}_j, \boldsymbol{\theta}) db_j$ ▷ EB for penalty

11: $\mathbf{b}^{t+1} \leftarrow p(\mathbf{b} | \bar{\boldsymbol{\beta}}, \mathbf{D}, \sigma_0^2, \hat{\boldsymbol{\theta}})$ ▷ Update latent space

12: $\sigma_{t+1}^2 = \arg \max_{\sigma^2} F(q_{\boldsymbol{\beta}}^{t+1}, q_{\mathbf{b}}^{t+1}, g^{t+1}, \sigma^2, \sigma_{0t}^2)_{\text{Nash}}$

13: $\sigma_{0t+1}^2 = \arg \max_{\sigma_0^2} F(q_{\boldsymbol{\beta}}^{t+1}, q_{\mathbf{b}}^{t+1}, g^{t+1}, \sigma_{t+1}^2, \sigma_0^2)_{\text{Nash}}$

14: $\omega_{t+1} = \frac{(n-1)\sigma_{0t+1}^2}{\sigma_{t+1}^2 + (n-1)\sigma_{0t+1}^2}$

15: $t \leftarrow t + 1$

16: **until** termination criterion is met

17: **return** $\bar{\mathbf{b}}, \boldsymbol{\pi}, \sigma^2$

B Nash optimizes a lower bound of mr.ash ELBO

The derivations below are adapted from Section 4.2.1 of Xie [2023]. While Xie [2023] studies a different problem (smoothing Poisson counts), we draw inspiration from this work and adapt it to the high-dimensional Gaussian setting. In this section, we show that in the absence of side information, Nash optimizes a lower bound of the mr.ash evidence lower bound (ELBO).

Recall the two models, mr.ash and Nash:

$$\begin{array}{cc} \text{mr.ash} & \text{Nash} & (49) \end{array}$$

$$\mathbf{y} | \mathbf{X}, \mathbf{b}, \sigma^2 \sim N(\mathbf{X}\mathbf{b}, \sigma^2) \quad \mathbf{y} | \mathbf{X}, \boldsymbol{\beta}, \sigma^2 \sim N(\mathbf{X}\boldsymbol{\beta}, \sigma^2) \quad (50)$$

$$b_j \sim g(\cdot) \quad \beta_j \sim N(b_j, \sigma_0^2) \quad (51)$$

$$b_j \sim g(\cdot) \quad (52)$$

We consider the case without side information, recall that both approach restrict their search to posteriors of the form

$$\begin{array}{cc} \text{mr.ash} & \text{Nash} & (53) \end{array}$$

$$q(\mathbf{b}) = \prod_j^P q_{b_j}(b_j) \quad q(\boldsymbol{\beta}, \mathbf{b}) = \prod_j^P q_{\beta_j}(\beta_j) q_{b_j}(b_j) \quad (54)$$

So the corresponding ELBO for the two models are

$$F(q_{\beta}, g; \sigma^2)_{mr.ash} = \sum_i \mathbb{E} \log \frac{p(y_i | \mathbf{x}_i, \mathbf{b}, \sigma^2)}{q_{\mathbf{b}}(\mathbf{b})} + \sum_j \mathbb{E} \log \frac{g(b_j)}{q_{b_j}(b_j)} \quad (55)$$

$$F(q_{\beta}, q_{\mathbf{b}}, g; \sigma^2 \sigma_0^2)_{Nash} = \sum_i \mathbb{E} \log \frac{p(y_i | \mathbf{x}_i, \beta, \sigma^2)}{q_{\beta}(\beta)} + \sum_j \mathbb{E} \log p(\beta_j | b_j, \sigma_0^2) + \sum_j \mathbb{E} \log \frac{g(b_j)}{q_{b_j}(b_j)} \quad (56)$$

Below we show that the profiled objective function $F(q_{\beta}, g; \sigma^2)_{Nash} = \max_{q_{\mathbf{b}}} F(q_{\beta}, q_{\mathbf{b}}, g; \sigma^2)_{Nash}$ is a lower bound for $F(q_{\beta}, g; \sigma^2)_{mr.ash}$.

B.1 Objective for b_j in the Nash model

The introduction of latent variable β_j induces a marginal density of b_j as

$$\log p(\mathbf{y} | \mathbf{x}, b_j, \sigma^2, \sigma_0^2) = \log \int p(\mathbf{y} | \mathbf{X}, \beta_j, \sigma^2) N(\beta_j, b_j, \sigma_0^2) g(b_j) d\beta_j \quad (57)$$

We denote $\log p(\mathbf{y} | \mathbf{x}, b_j, \sigma_0^2)$ by $\log f(b_j)$. Before demonstrating that Nash optimizes a lower bound for the mr.ash approximation, we first introduce a lemma.

Lemma *The second order derivative of $\log f(\cdot)$ with respect to b is lower bounded by $-1/\sigma_0^2$.*

Proof. The second derivative of $\log f(b)$ is

$$\frac{d^2 \log f(b_j)}{db_j^2} = \frac{f''(b_j)}{f(b_j)} - \left(\frac{f'(b_j)}{f(b_j)} \right)^2 \quad (58)$$

where

$$f'(b_j) = \frac{1}{\sigma_0^2} f(b_j) \int \beta p(\beta | b_j) g(b_j) d\beta - \frac{\beta}{\sigma_0^2} f(b_j) = \frac{1}{\sigma_0^2} f(b_j) (\mathbb{E}(\beta) - b_j),$$

$$f''(b_j) = \frac{1}{(\sigma_0^2)^2} f(b_j) (\mathbb{E}(\beta^2) - b_j \mathbb{E}(\beta)) - \frac{1}{\sigma_0^2} f'(b_j) - \frac{b_j}{\sigma_0^2} \quad (59)$$

$$= f(b_j) \left(\frac{1}{(\sigma_0^2)^2} \mathbb{E}(\beta^2) - \frac{2b_j}{(\sigma_0^2)^2} \mathbb{E}(\beta) - \frac{1}{\sigma_0^2} + \frac{b_j^2}{(\sigma_0^2)^2} \right) \quad (60)$$

where the expectation are under $p(\beta_j | y, \mathbf{X}, b_j, \sigma, \sigma_0^2)$

Substituting $f'(b_j)$ and $f''(b_j)$, we have

$$\frac{d^2 \log f(b_j)}{db_j^2} = -\frac{1}{\sigma_0^2} + \frac{1}{(\sigma_0^2)^2} (\mathbb{E}(\beta^2) - \mathbb{E}((\beta)^2)) \geq -\frac{1}{\sigma_0^2} \quad (61)$$

The primary objective is to perform inference on b_j , the most straightforward approach is to regard the marginal distribution as the prior of b_j and maximize the corresponding ELBO,

$$\tilde{F}(q_{\beta_j}, \sigma^2) = \mathbb{E} \log \frac{p(\mathbf{y} | \mathbf{X}, \beta_j, \beta_{-j})}{q_{\beta_j}} + \mathbb{E} \log f(\beta_j; g, \sigma^2). \quad (9)$$

The following theorem shows that the objective function maximized by the splitting approach is a lower bound of $F(q_{\beta_j}; \sigma^2)$.

Theorem B.1. *The profiled objective function $F(q_{b_j}; \sigma^2, \sigma_0^2) = \max_{q_{\beta_j}} F(q_{\beta_j}, q_{b_j}; \sigma^2, \sigma_0^2)_{Nash}$ is a lower bound of $F(q_{b_j}; \sigma^2)_{mr.ash}$.*

Proof. The ELBO of Nash for β_j, b_j is

$$F(q_{\beta_j}, q_{b_j}; \sigma^2, \sigma_0^2)_{Nash} = \mathbb{E} \log p(\mathbf{y} | \mathbf{X}, \beta_j, \boldsymbol{\beta}_{-j}) + \mathbb{E} \log \frac{N(\beta_j, \bar{b}_j, \sigma_0^2)}{q_{\beta_j}(\beta_j)} + \mathbb{E} \log \frac{g(b_j)}{q_{b_j}} - \frac{V_{q_{b_j}}}{2\sigma_0^2} \quad (62)$$

$$= \mathbb{E} \log p(\mathbf{r}_j | \mathbf{X}_j, \beta_j) + \mathbb{E} \log \frac{N(\beta_j, \bar{b}_j, \sigma_0^2)}{q_{\beta_j}(\beta_j)} + \mathbb{E} \log \frac{g(b_j)}{q_{b_j}} - \frac{V_{q_{b_j}}}{2\sigma_0^2} \quad (63)$$

Where $\mathbf{r}_j = \mathbf{y} - \mathbf{X}_{-j}\boldsymbol{\beta}_{-j}$, $\bar{b}_j = \mathbb{E}_{q_{b_j}}(b_j)$ and $V_{q_{b_j}} = \mathbb{E}_{q_{b_j}}(b - \bar{b})$

Therefore the profiled Nash ELBO for q_{b_j}, g is

$$F(b_j, g; \sigma^2, \sigma_0^2) = \max_{q_{\beta_j}} F(q_{\beta_j}, q_{b_j}; \sigma^2, \sigma_0^2)_{Nash} \quad (64)$$

$$= \log p(\mathbf{r}_j | \bar{b}_j, \sigma^2) + \mathbb{E} \log \frac{g(b_j)}{q_{b_j}} - \frac{V_{q_{b_j}}}{2\sigma_0^2} \quad (65)$$

The ELBO $F(q_{\beta_j}, q_{b_j}; \sigma^2, \sigma_0^2)_{Nash}$ reach its maximum over q_{β_j} at $q_{\beta_j}^* = p(\beta_j | \mathbf{r}_j, \bar{b}_j, \sigma_0^2)$

A second order Taylor series expansion of $F(q_{b_j}, g; \sigma^2)_{mr.ash}$ in around \bar{b}_j gives

$$F(q_{b_j}; \sigma^2)_{mr.ash} = \mathbb{E} \log p(\mathbf{y} | \mathbf{X}, b_j, \boldsymbol{\beta}_{-j}, \sigma^2, \sigma_0^2) + \mathbb{E} \log \frac{g(b)}{q_b} \quad (66)$$

$$= \log p(\mathbf{r}_{-j} | b_j, \sigma^2, \sigma_0^2) + \frac{1}{2} \left(\frac{d^2 f(b)}{db^2} \right) \Big|_{b=\bar{b}} V_{q_b} + \mathbb{E} \log \frac{g(b)}{q_b} \quad (67)$$

$$\geq \log p(\mathbf{r}_{-j} | b_j, \sigma^2, \sigma_0^2) - \frac{1}{2\sigma_0^2} V_{q_b} + \mathbb{E} \log \frac{g(b)}{q_b} \quad (68)$$

$$= \max_{q_{\beta_j}} F(q_{\beta_j}, q_{b_j}; \sigma^2, \sigma_0^2)_{Nash} \quad (69)$$

where θ is between $\hat{\beta}$ and β . The first inequality holds due to the Lemma above, and the second inequality is due to the definition of ELBO. \square

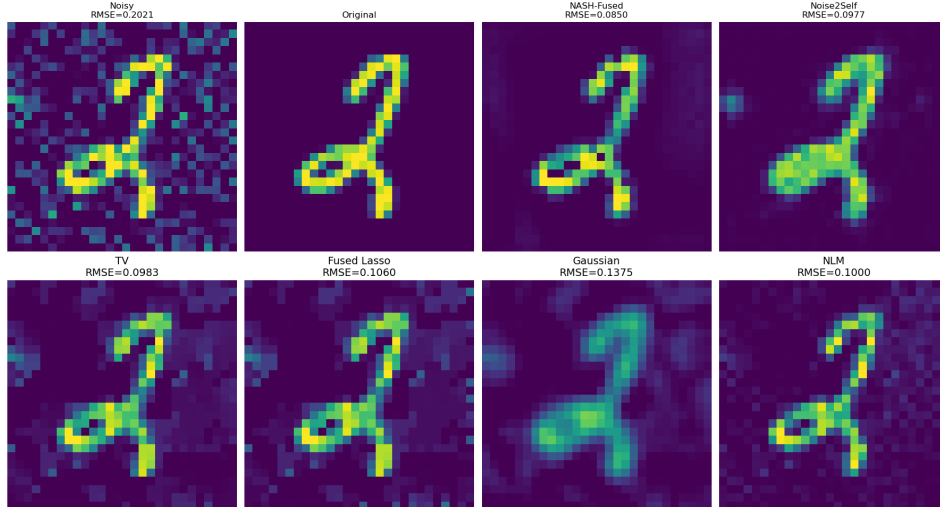


Figure 3: Additional denoised image

B.2 Real data experiment

MLP/Feed forward neural network: We trained a feedforward neural network (NN) as a baseline for comparison. The network consists of three fully connected layers: an input layer followed by two hidden layers of sizes 128 and 64, each with ReLU activation. The output is a single linear unit predicting a continuous response. The input features were standardized to zero mean and unit variance based on the training set. The model was trained using the Adam optimizer with a learning rate of 0.001 and mean squared error (MSE) loss. Each model was trained for 100 epochs using all training samples in batch mode. Training and evaluation were implemented in PyTorch. RMSE was computed on each test split, and average RMSE across the 10 folds is reported.

xgboost: We trained gradient-boosted decision trees using the xgboost *R* package with default hyperparameters. Specifically, we used roost mean square error as objective for regression. Each model was trained using 50 boosting iteration (default parameter) with a maximum tree depth of 6 and a learning rate (eta) of 0.3.

MNIST We evaluated seven denoising methods on the MNIST dataset with additive Gaussian noise of standard deviation $\sigma = 0.2$, applied independently to each pixel. Each method was applied to 20 randomly selected test images, and performance was measured using root mean squared error (RMSE) against the clean image. The Noise2Self model was a convolutional neural network (CNN) with three convolutional layers: $\text{Conv}_{1 \rightarrow 32} \rightarrow \text{ReLU} \rightarrow \text{Conv}_{32 \rightarrow 32} \rightarrow \text{ReLU} \rightarrow \text{Conv}_{32 \rightarrow 1}$. It was trained using masked pixel regression, where approximately 10% of pixels were randomly set to zero during each training iteration and the model was trained to reconstruct them. The loss was computed only over masked pixels using mean squared error. We trained the Noise2Self model for 5 epochs using the Adam optimizer with a learning rate of 10^{-3} and batch size 64.

The Nash-fused was trained using a message passing GNN representing each image as a 784-node graph corresponding to a 28×28 grid, with 4-neighbor connectivity and node features consisting of the noisy intensity and normalized spatial coordinates. The underlying graph neural network had two hidden layers with ReLU activations. We trained Nash-fused separately for each image using 300 steps of gradient descent with the Adam optimizer and learning rate 10^{-2} .

Classical baselines included total variation (TV) denoising, fused lasso, Gaussian smoothing, and non-local means (NLM). TV denoising used regularization weight 0.1. Fused lasso was formulated as a convex optimization problem with an ℓ_2 data fidelity term and isotropic TV penalty, solved using `cvxpy` with the SCS solver. Gaussian filtering used a fixed kernel with standard deviation $\sigma = 1$. NLM used the implementation from `skimage.restoration` with parameters $h = 1.15 \cdot \hat{\sigma}$ (where $\hat{\sigma}$ is estimated from the image), patch size 3, and patch distance 5.

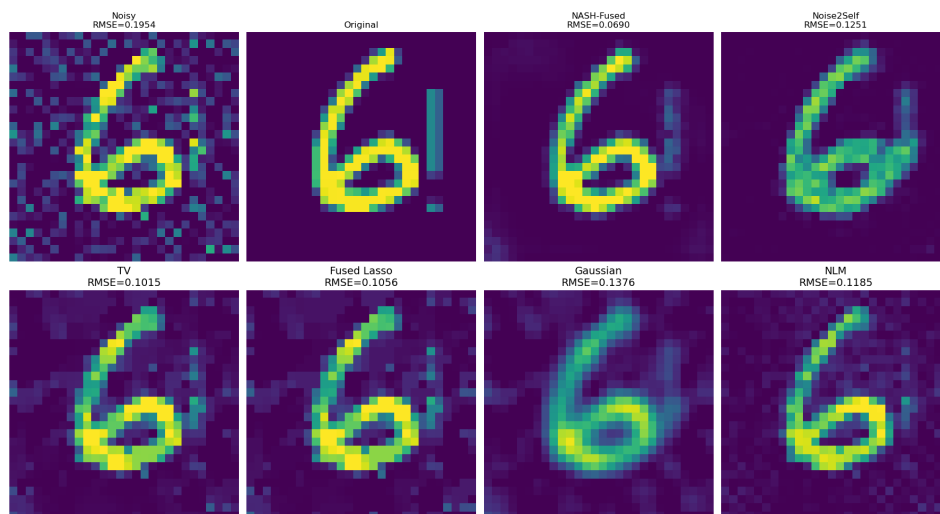


Figure 4: Additional denoised image

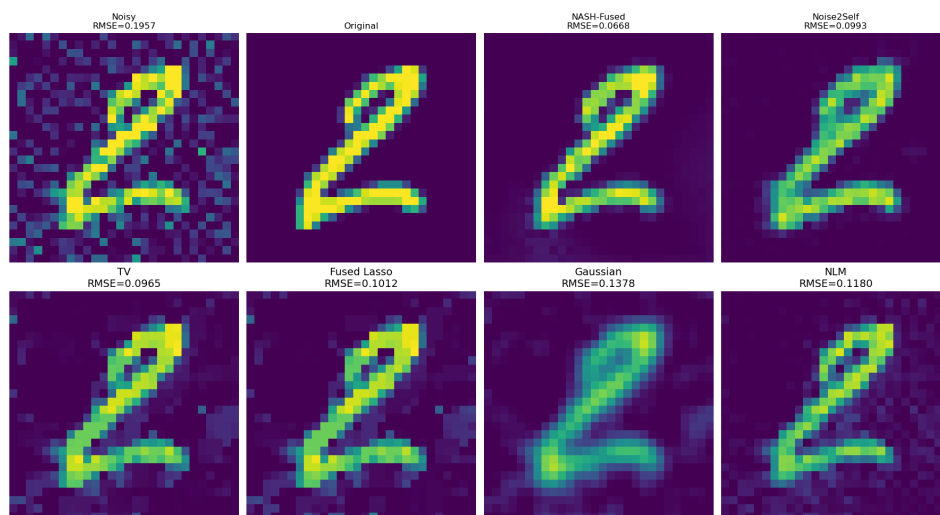


Figure 5: Additional denoised image

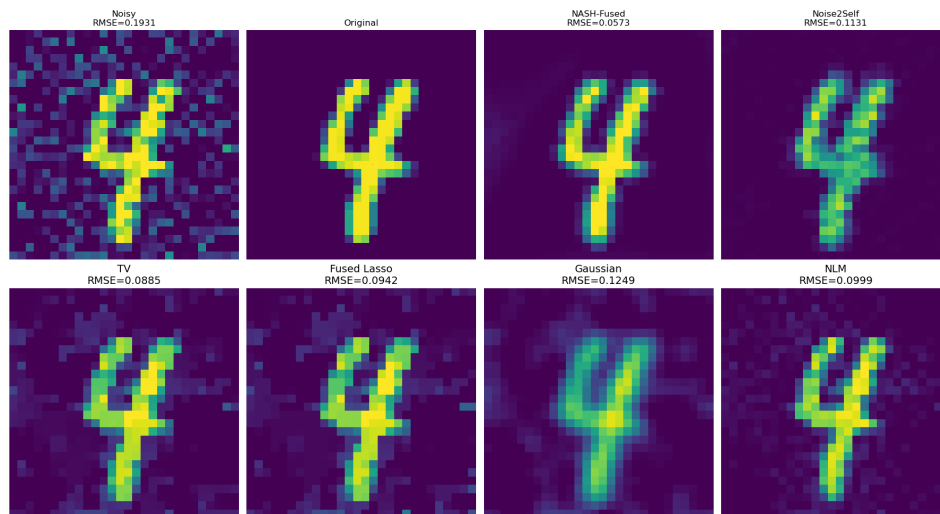


Figure 6: Additional denoised image

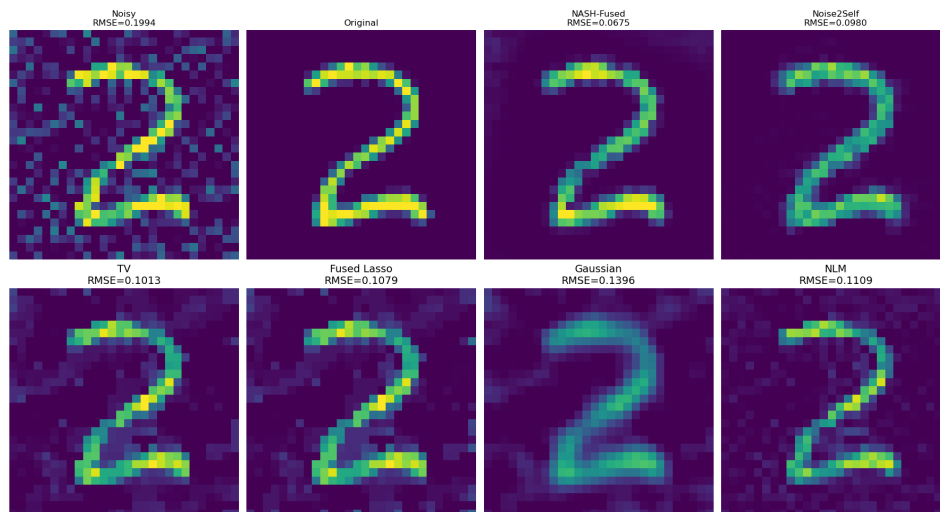


Figure 7: Additional denoised image

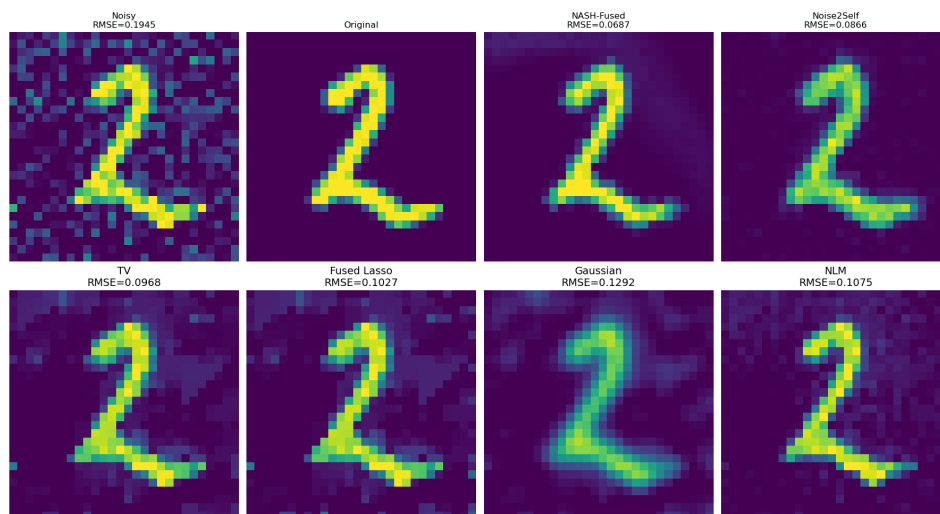


Figure 8: Additional denoised image

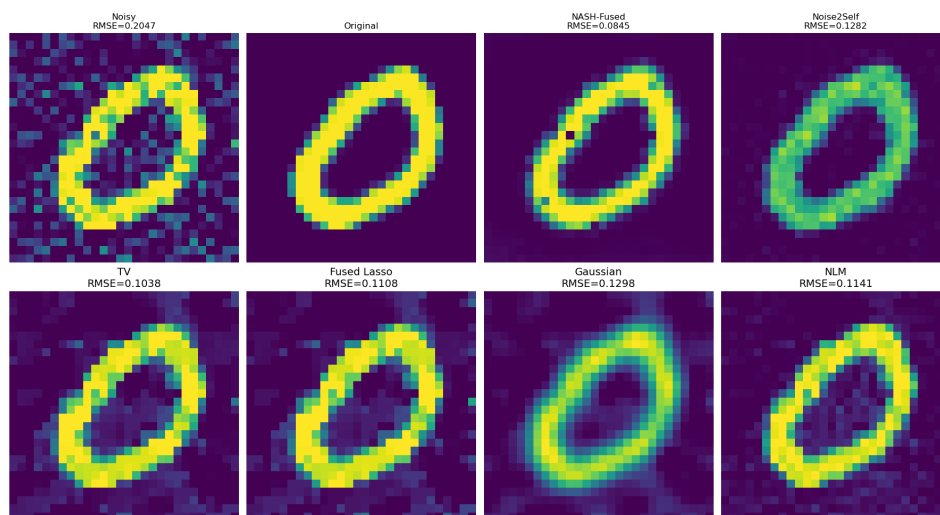


Figure 9: Additional denoised image